Water Oxidation

International Edition: DOI: 10.1002/anie.201601653
German Edition: DOI: 10.1002/ange.201601653

Self-Assembled Amphiphilic Water Oxidation Catalysts: Control of O–O Bond Formation Pathways by Different Aggregation Patterns

*Bing Yang, Xin Jiang, Qing Guo, Tao Lei, Li-Ping Zhang, Bin Chen, Chen-Ho Tung, and Li-Zhu Wu**

Abstract: *The oxidation of water to molecular oxygen is the key step to realize water splitting from both biological and chemical perspective. In an effort to understand how water oxidation occurs on a molecular level, a large number of molecular catalysts have been synthesized to find an easy access to higher oxidation states as well as their capacity to make O–O bond. However, most of them function in a mixture of organic solvent and water and the O–O bond formation pathway is still a subject of intense debate. Herein, we design the first amphiphilic Ru-bda (H_2bda = 2,2′-bipyridine-6,6′-dicarboxylic acid) water oxidation catalysts (WOCs) of formula [Ru^{II}(bda)(4-OTEG-pyridine)$_2$] (**1**, OTEG = $OCH_2CH_2OCH_2CH_2OCH_3$) and [Ru^{II}(bda)($PySO_3Na$)$_2$] (**2**, $PySO_3^-$ = pyridine-3-sulfonate), which possess good solubility in water. Dynamic light scattering (DLS), scanning electron microscope (SEM), critical aggregation concentration (CAC) experiments and product analysis demonstrate that they enable to self-assemble in water and form the O–O bond through different routes even though they have the same bda^{2-} backbone. This work illustrates for the first time that the O–O bond formation pathway can be regulated by the interaction of ancillary ligands at supramolecular level.*

To meet the sustainable production of clean energy demands, water splitting into molecular oxygen and hydrogen has become one of the most attractive strategies.[1] The whole water splitting process consists of two half reactions: the proton reduction and the water oxidation. The former half reaction is less energy demanding compared with the latter one, which is the key step and is always considered as a bottleneck because it requires the transfer of four electrons and formation of the O–O bond.[2,3] Over the past decades, a great quantity of molecular catalysts in relation to mono-, di-, and polynuclear Ru-,[4–27] Ir-,[28,29] Mn-,[30–32] Co-,[33–36] Fe-[37–39] and Cu-based[40–44] metal complexes have been developed. Among them, Ru-based WOCs are the most representative. Particularly, Sun and co-workers reported in 2012 a set of quite efficient catalysts bearing the tetradentate bda^{2-} as equatorial ligand and having a maximal TOF value of 303.0 s^{-1} (complex **3**, see Scheme 1),[14] which was even comparable with that of oxygen evolution complex (OEC) in photosystem II (PSII).[45] Despite this progress, the comprehensive understanding of the reaction pathways for O–O bond formation, together with the full spectroscopic characterization of reaction intermediates, is a huge challenge.

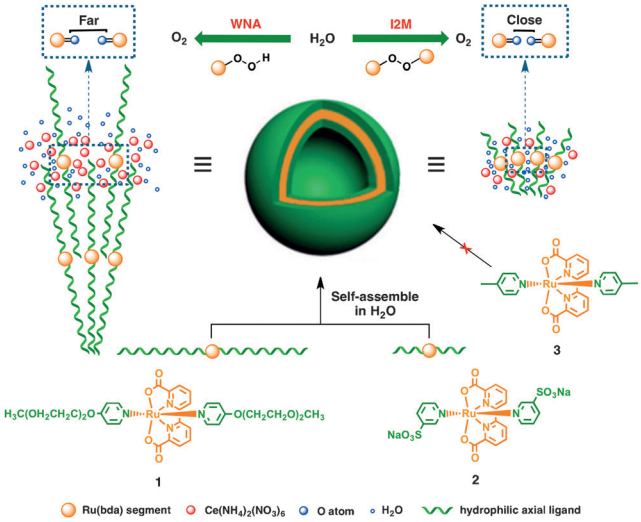

Scheme 1. Subtle supramolecular interactions regulate the O–O bond formation pathways for amphiphilic WOCs of **1** and **2** in water.

It is generally accepted two different pathways with regard to the O–O bond formation, namely water nucleophilic attack (WNA), and interaction of two higher oxidation state of M–O units (I2M).[19] But there is still no final evidence in favor of WNA or I2M no matter for natural PSII or the synthetic transition-metal complexes. Till now, most of the synthetic Ru-based water oxidation systems adopt WNA except Ru-bda type catalysts reported by Sun and co-workers[14,18] and several other binuclear WOCs that undergo intramolecular I2M pathway.[6,16] Furthermore, almost all the reported catalysts function in the presence of organic solvent, which might lead to undesired deactivation pathways and increase the complexity of an already very complex reaction since the high thermodynamic redox potential needed for water oxidation permits the catalyst to oxidize a broad range of organic and inorganic substrates.

In 2014 Llobet and co-workers revealed that WNA and I2M pathways had relatively close activation energy barriers and the O–O bond formation mechanism would be influenced by changing equatorial ligand constrains.[19] Such

[*] B. Yang, X. Jiang, Q. Guo, T. Lei, Prof. Dr. L.-P. Zhang, Dr. B. Chen, Prof. Dr. C.-H. Tung, Prof. Dr. L.-Z. Wu
Key Laboratory of Photochemical Conversion and Optoelectronic Materials, Technical Institute of Physics and Chemistry & University of Chinese Academy of Sciences, Chinese Academy of Sciences
Beijing 100190 (P.R. China)
E-mail: lzwu@mail.ipc.ac.cn

Supporting information for this article can be found under: http://dx.doi.org/10.1002/anie.201601653.

a mechanistic variation from I2M to WNA was also observed when Ru-bda WOC was covalently anchored on a solid surface.[27] Inspired by these findings, we wonder whether we could take advantage of supramolecular interactions to modulate the molecular arrangement and distance of WOCs, and further modulate the O−O bond formation pathways for water oxidation. Given that amphiphiles possess good solubility and are able to self-assemble in water,[46–49] we introduce here the first set of amphiphilic WOCs, which contain both hydrophilic ether chain or sulfonate as axial ligands and a hydrophobic bda^{2-} segment as equatorial ligand (**1** and **2**, see Scheme 1). Because of the different length and structure of these two axial ligands, it is anticipated that complexes **1** and **2** could be ideal models to probe the water oxidation mechanism regulated by supramolecular interactions of axial ligands. Indeed, such design successfully executes our plans.

The synthesis of complexes **1** and **2** was achieved by reaction of 2,2′-bipyridine-6,6′-dicarboxylic acid and Ru-$(DMSO)_4Cl_2$ in the presence of methanol/triethylamine, and then addition of excess water soluble axial ligands. Both of the complexes were fully characterized by ^{1}H NMR and HRMS spectrometry (see Figure S1–S3 in the Supporting Information), UV/Vis absorption and electrochemical spectra. Complex **3** was also prepared for comparison.

Complexes **1** and **2** were soluble in water and the solubility was determined to be 1.58 mM for **1** and 48.46 mM for **2**, respectively (see Figure S4–S7). UV/Vis absorption spectra of complexes **1** and **2** in different solvents were then examined. As shown in Figure 1, complex **1** displayed two peaks at

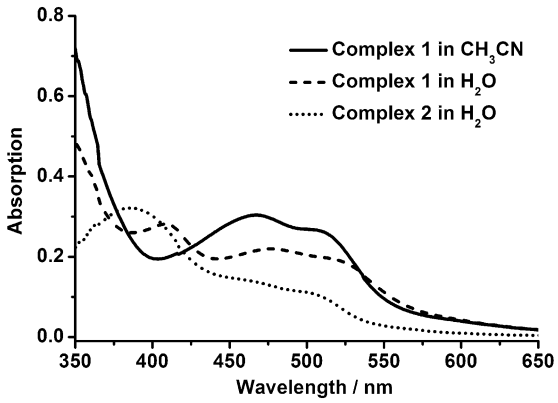

Figure 1. The UV/Vis absorption spectra of complex **1** in acetonitrile (solid line) and water (dash line), and complex **2** in water (dot line). The concentration of complexes **1** and **2** is 1.0×10^{-4} mol L^{-1}.

460 nm and 510 nm in acetonitrile solution, typical from MLCT [d(Ru)→π*(bipyridine) and π*(pyridine)] states.[25] In contrast to the fact, i.e., the energy of charge transfer bands increases with solvent polarity,[50] the aqueous solution of complex **1** showed weaker and bathochromic-shifted absorptions at 480 and 530 nm. This implied the aggregation behavior of amphiphilic complex **1** in water.[50] As for complex **2**, the experiment was carried out only in water because of its poor solubility in organic solvent. With reference to the spectroscopic study on Ru-based WOCs,[8] the strong peak at 390 nm was assigned to the absorption of ILCT state between the axial and equatorial ligands, and the 450–520 nm peaks were tentatively ascribed to its MLCT absorption. Simultaneously, control experiment of complex **3** was conducted in acetonitrile. When adding water to its acetonitrile solution, the peaks at 405 nm and 550 nm moved to 380 nm and 500 nm, respectively (see Figure S8). The blue shift was in line with the polarity change of solvents from acetonitrile to water,[50] suggesting that complex **3** did not aggregate in water, but complexes **1** and **2** did.

The aggregation behaviors were further investigated by SEM and DLS measurements. The SEM images showed that complexes **1** and **2** aggregated into vesicle-like spherical particles in water with diameters around 100 nm, which were in accordance with the DLS results (see Figure 2). By

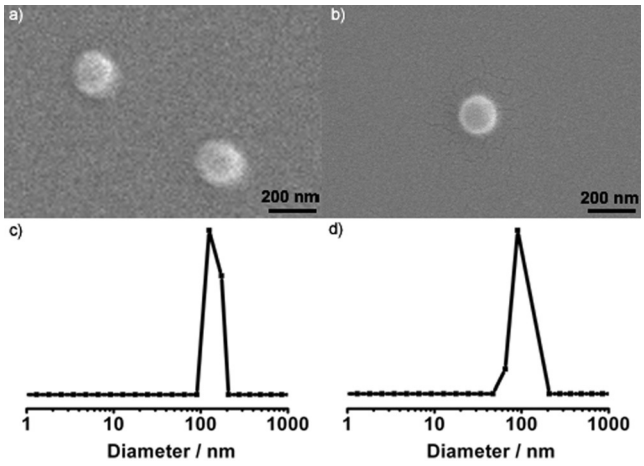

Figure 2. SEM images of the aggregations and DLS analysis of complex **1** (a, c) and **2** (b, d) in water. The concentrations of complexes for SEM and DLS are 2.0×10^{-4} and 1.5×10^{-5} mol L^{-1}, respectively.

contrast, the acetonitrile solutions of complexes **1** and **2** and the aqueous solution of complex **3** showed no particle size distributions from 0 to 1000 nm, further confirming that complexes **1** and **2** self-assembled just in water. The critical aggregation concentration (CAC) of complexes **1** and **2** was then determined by the fluorescent method. Due to strong hydrophobicity, organic dye Nile red (NR) shows no absorption and fluorescence in water. But when the concentration of complexes is higher than the CAC, the NR would like to go inside of the aggregates to show strong fluorescence.[50] In the current case, the fluorescence of NR was found strong even at the concentrations of **1** and **2** being low to 10^{-8} mol L^{-1}. While under the same condition, the aqueous solution of NR showed no fluorescence at all (see Figure S9–S10). These results meant that both complexes existed as the aggregation forms in water. In addition, the UV/Vis absorption curves for both complexes **1** and **2** kept unchanged over a time period of 24 hours, indicating the structural integrity of the aggregates formed by **1** and **2** in water (see Figure S11–S12).

Cyclic voltammery (CV) were used to electrochemically characterize complexes **1** and **2** in 0.1M HNO_3 aqueous

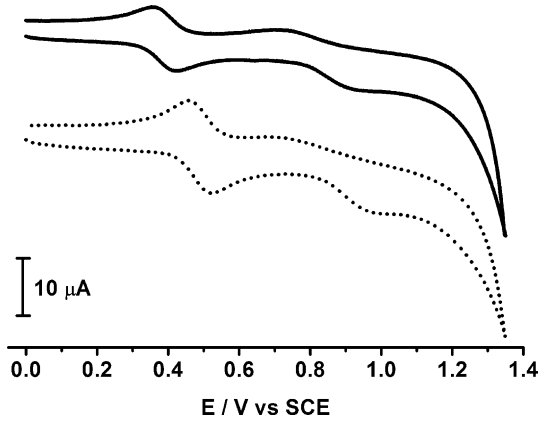

Figure 3. CV curves of complex **1** (solid line) and **2** (dot line) in 0.1 mol L^{-1} HNO_3 aqueous solution on a glassy carbon disk working electrode using Pt wire as an auxiliary and SCE as reference electrode at a scan rate of 50 mV s^{-1}. The concentration of complexes **1** and **2** is 1.0×10^{-3} mol L^{-1}, and the concentration of NaCl is 0.1 mol L^{-1}.

solution at pH 1. As shown in Figure 3, two reversible couples ($|ipa/ipc|=1$) at 0.42 and 0.52 V vs. SCE (saturated calomel electrode) for complexes **1** and **2** were corresponding to the $Ru^{III/II}$ process. The peak value for complex **2** was slightly higher than that for complex **1** because of the presence of electron withdrawing sulfonate groups. Both of the values of $Ru^{III/II}$ couples were independent on the pH change (see Figure S13–S14), implying proton transfer was not involved in this process. The quasi-irreversible waves at 0.92 and 0.98 V vs. SCE for **1** and **2** were assigned to the $Ru^{IV/III}$ redox couples, but the $Ru^{V/IV}$ peak was not observed. Perhaps the $Ru^{IV/V}$ peak was contained in the next onset of a catalytic water oxidation wave since the value of this redox couple usually appears over 1.30 V vs. SCE.[9,17] The two large anodic electrocatalytic peaks around 1.30 V vs. SCE for complexes **1** and **2** were associated with the catalytic water oxidation process with an overpotential of 0.37 V ($E=0.93$ V vs. SCE at pH 1) because the high valence Ru species were able to form the Ru-O-O-X (X = H or Ru) intermediates, thus leading to molecular oxygen evolution via electrochemical process.

Next, the ability of complexes **1** and **2** to act as catalyst for oxygen evolution was evaluated using CAN as sacrificial oxidant. An aqueous solution of each catalyst was added to the CAN aqueous solution and stirred at room temperature. The amount of oxygen evolution was then monitored using the method of water displacement. System **1** (0.2 mM)/CAN (0.46 M) gave an impressive TON of 1300 with an initial TOF of 10 s^{-1}. Under the same conditions, complex **2** gave a TON of 800 with a similar initial TOF value to **1** (see Figure S15). Recent study by Masaoka and co-workers revealed that the pendant SO_3^- groups on the catalyst could capture CAN to enhance its activity.[25] In our **2**/CAN water oxidation system, however, the CAN concentration was so high that the assistance of pendant SO_3^- groups of complex **2** was negligible if there was any in the water oxidation system.

For single-site Ru WOCs, it has been known that a high valence Ru species $Ru^V{=}O$[4,7–11,13] or $Ru^{IV}{=}O$[12] intermediate must be formed to either react with water molecule or couple with another high valence Ru=O species for the O–O bond formation. To shed light on the Ru intermediate, electron paramagnetic resonance (EPR) was employed as it is unique to identify the paramagnetic intermediates: Ru^{III} (d^5) and Ru^V (d^3) complexes.[21] Upon addition of 1 equiv of CAN into the aqueous solution of complex **1**, the paramagnetic Ru^{III} species with $g_{xx}=2.285$, $g_{yy}=2.093$, and $g_{zz}=1.991$ emerged immediately (see Figure 4a, dot line). After adding excess (20 equiv)

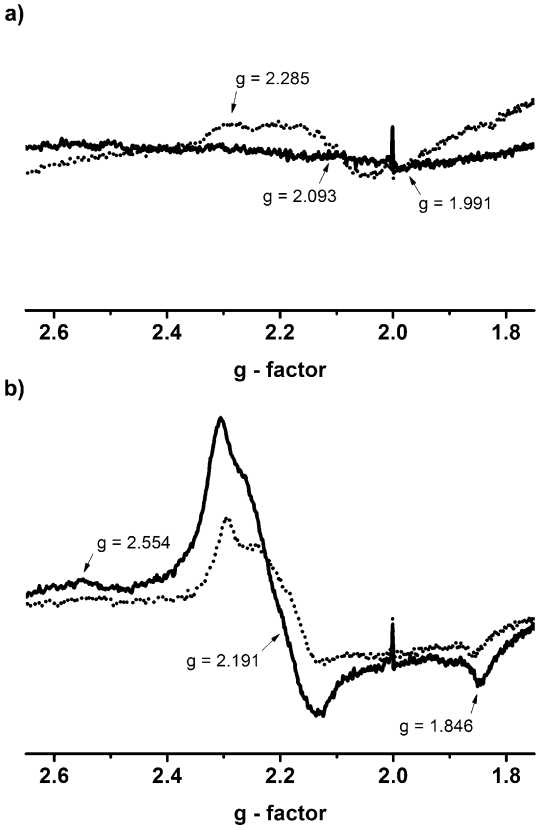

Figure 4. X-Band EPR spectra (90 K) of 1.0×10^{-3} mol L^{-1} aqueous solution of Ru^{III} species (dot line) and catalytic mixture (solid line) generated by adding 20 equiv of CAN to the 1.0×10^{-3} mol L^{-1} aqueous solution of complex **1** (a) and complex **2** (b), respectively. The peak around $g=2.0$ is from the EPR instrument.

of CAN and freezing within 30 s, complex **1** underwent further oxidation to afford EPR silent form, indicating that the $Ru^{IV}=O$ rather than $Ru^V{=}O$ species was formed in the catalytic steady state for complex **1** (see Figure 4a, solid line). Similarly, upon addition of 1 equiv of CAN into the aqueous solution of complex **2**, the paramagnetic Ru^{III} species was formed (see Figure 4b, dot line). After addition of 20 equiv CAN to complex **2** and freezing within 30 s, however, the solid line in Figure 4b showed the signal of a mixture of Ru^{III} and Ru^V species with a new g value of 2.554.[21,51–53] Obviously, complexes **1** and **2** went through different high valence state of Ru species during the water oxidation process. This is probably due to the fact that the sulfonate group has stronger electron-withdrawing ability than the ether chain, and would stabilize the high valence Ru center to allow for the formation of Ru^V species.

Given the fact that the O–O bond formation process is always considered as the rate-determining step,[4,8] it is of significance to figure out how the O–O bond is formed and what factors determine the O–O bond formation pathway. To this end, we measured the initial rate of oxygen evolution of complexes **1** and **2** as a function of catalyst concentration by Clark oxygen electrode (see Figure 5). On the basis of the

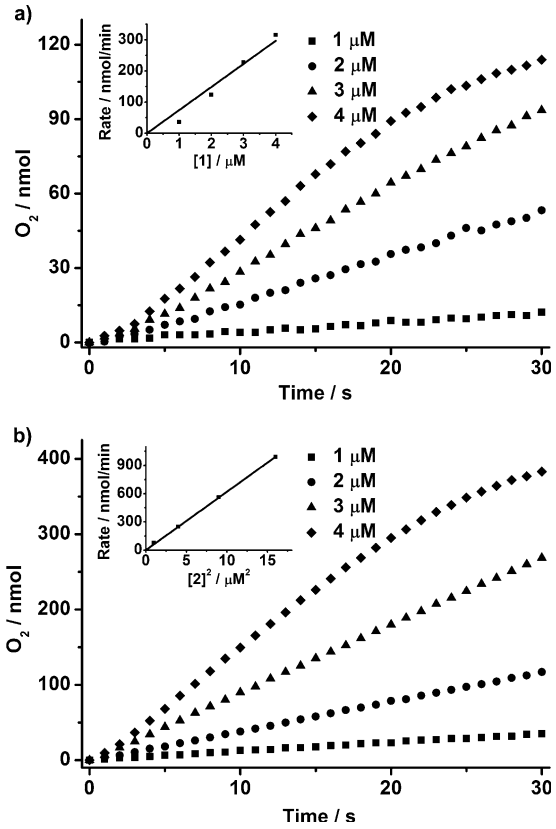

Figure 5. Oxygen evolution recorded by Clark oxygen electrode. Conditions: 2.0 mL aqueous solution containing 1.0×10^{-2} mol L^{-1} CAN and catalyst **1** (a) and **2** (b) of different concentrations. Inset, plot of the initial O_2 evolution rate versus [**1**] (a) and [**2**]^2 (b).

amount of oxygen evolution at the beginning time of 5 seconds, we calculated the initial rate for oxygen generation. The results showed that a linear relationship ($R^2 = 0.98$) would be maintained when the concentration of **1** was plotted against the initial rate of oxygen evolution. This is a typical feature of a mononuclear WNA pathway for the O–O bond formation. Different from complex **1**, if the concentration square of **2** was plotted against the initial rate for oxygen evolution, we obtained a linear correlation ($R^2 = 0.99$), showing a different bimolecular I2M mechanism.

It was worth noting the diverse O–O bond formation pathways for complexes **1** and **2** because they had almost the same molecular scaffold but only different in axial ligands. Combining with EPR, concentration-rate relationship results and the fact that Ru-bda type catalysts tend to form the seven coordinated Ru-OH_2 species because of the large O-Ru-O angle of 123.1°,[14] we tentatively proposed different mechanisms for complexes **1** and **2** (see Scheme 2). Firstly, the Ru^{II}-

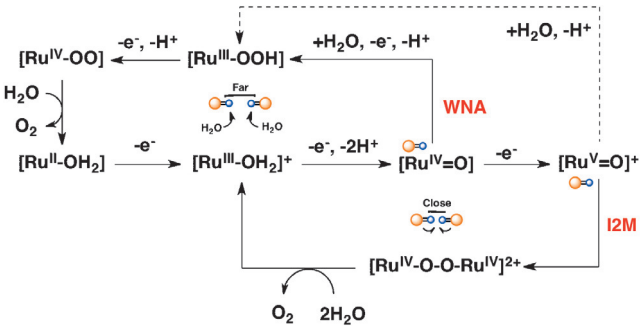

Scheme 2. Proposed water oxidation mechanisms catalyzed by complexes **1** and **2**. The dash line represents another possible pathway that is not observed in this work.

WOCs associates with a molecule of water to form a seven coordinated Ru^{II}-OH_2 species, which is oxidized by CAN to Ru^{III}-OH_2 and then to higher valence Ru^{IV}=O intermediates through the proton coupled electron transfer (PCET) process. The Ru^{IV}=O can be further oxidized to Ru^{V}=O by excess CAN, and the generated higher valence Ru^{V}=O species may survive under suitable conditions.[9] Depending on the characteristics of molecular Ru-WOCs, the obtained Ru^{IV}=O or Ru^{V}=O species can thus form the O–O bond through WNA or I2M pathways. For complex **1**, Ru^{IV}=O species detected is attacked by a molecule of water to form the O–O bond through a mononuclear pathway. While for complex **2**, a higher valence Ru^{V}=O species is formed for the O–O bond formation via a bimolecular process. Our results showed that the axial ligands and aggregation patterns could contribute to higher oxidation states of Ru-WOCs and subsequently modulate the O–O bond formation mechanism. Although early studies have demonstrated that axial ligands are capable of improving the activity[14,18,22] and longevity[17] of WOCs by means of π–π stacking effect and increasing binding affinity between ligands and the metal center, this is, to the best of our knowledge, the first example showing that the aggregated molecular catalysts with different axial ligands may lead to the O–O bond formation pathway variation.

The unlike nature of hydrophilic axial ligands for complexes **1** and **2** caused different supramolecular interaction modes, and the different interaction modes would further lead to varying O–O bond formation pathways. To be specific, for complex **1**, the long ether chains tend to pile up and twist with each other and thus complex **1** adopts an intervalic aggregation mode in water.[50,54] As a consequence, the ligand can get close to the most extent and the distance between two Ru^{IV}=O metal centers is enlarged for **1**, resulting in the formation of O–O bond through WNA mechanism (see Scheme 1 and Scheme 2). As for complex **2**, the hydrophilic sulfonate part is relatively shorter than that of **1**, and tends to aggregate of the stabilized higher valence state of Ru species, where the hydrophilic sulfonate ligands pile with each other so that the two Ru^{V}=O centers get into proximity easily and form the O–O bond through the I2M mechanism (see Scheme 1 and Scheme 2).

In summary, we present two kinds of amphiphilic Ru-based complexes bearing different hydrophilic axial ligands,

which are able to catalyze water oxidation in pure water, and the cumulate water-soluble ligands lead to subtle arrangements and subsequently diverse O–O bond formation pathways. This finding demonstrates for the first time that noncovalent supramolecular interaction would influence the water oxidation mechanism, thus providing important piece of information to acquire comprehensive insights into the water oxidation process. Study on oxygen evolution from an assembling perspective not only helps understanding the mechanism for O–O bond formation, but also gains insight into the reaction center in PSII, a supramolecular environment for oxygen generation in natural photosynthesis.

Experimental Section

All reagents and solvents used in the present work were obtained commercially without further purification if there was no special notification. The equatorial and axial ligands were prepared as described in the Supporting Information.

[Ru(bda)(4-OTEG-pyridine)$_2$] (**1**). A mixture of 2,2′-bipyridine-6,6′-dicarboxylic acid (24.4 mg, 0.1 mmol), Ru(DMSO)$_4$Cl$_2$ (48.4 mg, 0.1 mmol) and NEt_3 (0.2 mL) in methanol (20 mL) was degassed with Ar and refluxed over 2 h. An excess of 4-OTEG-pyridine (0.22 g, 1 mmol) was added and the reflux was continued overnight. The solvent was removed and the residual solid was purified by column chromatography on silica gel using DCM-methanol (80/1 to 30/1, v/v) as eluents, **1** was obtained as red-brown solid (32.7 mg, 44.4% yield). ^{1}H-NMR (400 MHz, $CDCl_3$): $\delta = 8.12$ (s, 4H), 7.65 (s, 2H), 7.52 (s, 4H), 6.55 (s, 4H), 4.05 (s, 4H), 3.76 (s, 4H), 3.62 (s, 4H), 3.50 (s, 4H), 3.33 ppm (s, 6H). HRMS (ESI$^+$) *m*/*z* calculated for $C_{32}H_{36}N_4O_{10}Ru$ $[M+H]^+$ 739.1553, found 739.1546.

[Ru(bda)(PySO$_3$Na)$_2$] (**2**). A mixture of 2,2′-bipyridine-6,6′-dicarboxylic acid (244 mg, 1 mmol), Ru(DMSO)$_4$Cl$_2$ (484 mg, 1 mmol) and NEt_3 (0.8 mL) in methanol (30 mL) was degassed with Ar and refluxed overnight. The reaction mixture was cooled to room temperature and the resting red precipitate Ru(bda)(DMSO)$_2$ was collected and washed with methanol and dried (262 mg, 52.5% yield). A mixture of Ru(bda)(DMSO)$_2$ (50 mg, 0.1 mmol), pyridine-3-sulfonic acid (159 mg, 1 mmol) and Na_2CO_3 (106 mg, 1 mmol) in methanol (30 mL) was degassed with Ar and refluxed overnight. The solvent was removed and the residual solid was purified by column chromatography on silica gel using DCM-methanol (3/2, v/v) as eluents, **2** was obtained as red solid (44 mg, 62.3%). ^{1}H-NMR (400 MHz, D_2O): $\delta = 8.59$ (dd, $J = 7.0$, 2.2 Hz, 2H), 8.26 (d, $J =$ 5.6 Hz, 2H), 8.05–7.95 (m, 6H), 7.92 (s, 2H), 7.39 ppm (dd, $J = 8.0$, 5.8 Hz, 2H). HRMS (ESI$^-$) *m*/*z* calculated for $C_{22}H_{14}N_4O_{10}RuS_2$ $[M-2Na]^{2-}$ 329.9598, found 329.9604.

A typical procedure for a catalysis measurement using the method of displacement of water is as follows: 1.0 g $Ce(NH_4)_2(NO_3)_6$ was dissolved in 3.5 mL water and then an aqueous solution of catalyst (0.5 mL, 1.6×10^{-3} mol L^{-1}) was immediately injected to the CAN solution under vigorous stirring. The generated O_2 was measured through the numerical reading variation of the upside-down burette, which was connected to the sealed reaction bottle by a very thin pipe.

A typical procedure for a catalysis measurement using Hansatech Oxygraph is as follows: 2.0 mL 0.01 mol L^{-1} CAN aqueous solution was placed in the reaction chamber of the Clark oxygen electrode and then an aqueous solution of catalyst (1–5 μL, 2 mM) was injected to the CAN solution under stirring. The amount of generated O_2 and the water oxidation reaction rate were recorded by the Clark oxygen electrode.

Acknowledgements

This work was supported by the Ministry of Science and Technology of China (2013CB834505, 2014CB239402, and 2013CB834804), the National Natural Science Foundation of China (91427303, 21390404, and 51373193), the Key Research Programme of the Chinese Academy of Sciences (KGZD-EW-T05) and the Chinese Academy of Sciences.

Keywords: amphiphilic complexes · catalysis · ruthenium complex · self-assembly · water oxidation

How to cite: *Angew. Chem. Int. Ed.* **2016**, *55*, 6229–6234
Angew. Chem. **2016**, *128*, 6337–6342

[1] J. H. Alstrum-Acevedo, M. K. Brennaman, T. J. Meyer, *Inorg. Chem.* **2005**, *44*, 6802–6827.
[2] S. Romain, L. Vigara, A. Llobet, *Acc. Chem. Res.* **2009**, *42*, 1944–1953.
[3] J. J. Concepcion, J. W. Jurss, M. K. Brennaman, P. G. Hoertz, A. O. T. Patrocinio, N. Y. Murakami Iha, J. L. Templeton, T. J. Meyer, *Acc. Chem. Res.* **2009**, *42*, 1954–1965.
[4] J. J. Concepcion, J. W. Jurss, J. L. Templeton, T. J. Meyer, *J. Am. Chem. Soc.* **2008**, *130*, 16462–16463.
[5] Y. V. Geletii, Z. Huang, Y. Hou, D. G. Musaev, T. Lian, C. L. Hill, *J. Am. Chem. Soc.* **2009**, *131*, 7522–7523.
[6] S. Romain, F. Bozoglian, X. Sala, A. Llobet, *J. Am. Chem. Soc.* **2009**, *131*, 2768–2769.
[7] D. J. Wasylenko, C. Ganesamoorthy, M. A. Henderson, B. D. Koivisto, H. D. Osthoff, C. P. Berlinguette, *J. Am. Chem. Soc.* **2010**, *132*, 16094–16106.
[8] J. J. Concepcion, M.-K. Tsai, J. T. Muckerman, T. J. Meyer, *J. Am. Chem. Soc.* **2010**, *132*, 1545–1557.
[9] J. J. Concepcion, J. W. Jurss, M. R. Norris, Z. Chen, J. L. Templeton, T. J. Meyer, *Inorg. Chem.* **2010**, *49*, 1277–1279.
[10] L.-P. Wang, Q. Wu, T. Van Voorhis, *Inorg. Chem.* **2010**, *49*, 4543–4553.
[11] T. F. Hughes, R. A. Friesner, *J. Phys. Chem. B* **2011**, *115*, 9280–9289.
[12] D. E. Polyansky, J. T. Muckerman, J. Rochford, R. Zong, R. P. Thummel, E. Fujita, *J. Am. Chem. Soc.* **2011**, *133*, 14649–14665.
[13] L. Vigara, M. Z. Ertem, N. Planas, F. Bozoglian, N. Leidel, H. Dau, M. Haumann, L. Gagliardi, C. J. Cramer, A. Llobet, *Chem. Sci.* **2012**, *3*, 2576–2586.
[14] L. Duan, F. Bozoglian, S. Mandal, B. Stewart, T. Privalov, A. Llobet, L. Sun, *Nat. Chem.* **2012**, *4*, 418–423.
[15] T. Wada, H. Ohtsu, K. Tanaka, *Chem. Eur. J.* **2012**, *18*, 2374–2381.
[16] S. Maji, L. Vigara, F. Cottone, F. Bozoglian, J. Benet-Buchholz, A. Llobet, *Angew. Chem. Int. Ed.* **2012**, *51*, 5967–5970; *Angew. Chem.* **2012**, *124*, 6069–6072.
[17] L. Duan, C. M. Araujo, M. S. G. Ahlquist, L. Sun, *Proc. Natl. Acad. Sci. USA* **2012**, *109*, 15584–15588.
[18] L. Wang, L. Duan, Y. Wang, M. S. Ahlquist, L. Sun, *Chem. Commun.* **2014**, *50*, 12947–12950.
[19] S. Neudeck, S. Maji, I. Lopez, S. Meyer, F. Meyer, A. Llobet, *J. Am. Chem. Soc.* **2014**, *136*, 24–27.
[20] M. Hansen, F. Li, L. Sun, B. König, *Chem. Sci.* **2014**, *5*, 2683–2687.
[21] Y. Pushkar, D. Moonshiram, V. Purohit, L. Yan, I. Alperovich, *J. Am. Chem. Soc.* **2014**, *136*, 11938–11945.
[22] C. J. Richmond, R. Matheu, A. Poater, L. Falivene, J. Benet-Buchholz, X. Sala, L. Cavallo, A. Llobet, *Chem. Eur. J.* **2014**, *20*, 17282–17286.

[23] H. Li, F. Li, B. Zhang, X. Zhou, F. Yu, L. Sun, *J. Am. Chem. Soc.* **2015**, *137*, 4332 – 4335.
[24] V. Kunz, V. Stepanenko, F. Wurthner, *Chem. Commun.* **2015**, *51*, 290 – 293.
[25] M. Yoshida, M. Kondo, S. Torii, K. Sakai, S. Masaoka, *Angew. Chem. Int. Ed.* **2015**, *54*, 7981 – 7984; *Angew. Chem.* **2015**, *127*, 8092 – 8095.
[26] R. Matheu, M. Z. Ertem, J. Benet-Buchholz, E. Coronado, V. S. Batista, X. Sala, A. Llobet, *J. Am. Chem. Soc.* **2015**, *137*, 10786 – 10795.
[27] R. Matheu, L. Francàs, P. Chernev, M. Z. Ertem, V. Batista, M. Haumann, X. Sala, A. Llobet, *ACS Catal.* **2015**, *5*, 3422 – 3429.
[28] N. D. McDaniel, F. J. Coughlin, L. L. Tinker, S. Bernhard, *J. Am. Chem. Soc.* **2008**, *130*, 210 – 217.
[29] O. Diaz-Morales, T. J. Hersbach, D. G. Hetterscheid, J. N. Reek, M. T. Koper, *J. Am. Chem. Soc.* **2014**, *136*, 10432 – 10439.
[30] J. Limburg, *Science* **1999**, *283*, 1524 – 1527.
[31] E. A. Karlsson, B. L. Lee, T. Akermark, E. V. Johnston, M. D. Karkas, J. Sun, O. Hansson, J. E. Backvall, B. Akermark, *Angew. Chem. Int. Ed.* **2011**, *50*, 11715 – 11718; *Angew. Chem.* **2011**, *123*, 11919 – 11922.
[32] B. Nepal, S. Das, *Angew. Chem. Int. Ed.* **2013**, *52*, 7224 – 7227; *Angew. Chem.* **2013**, *125*, 7365 – 7368.
[33] Q. Yin, J. M. Tan, C. Besson, Y. V. Geletii, D. G. Musaev, A. E. Kuznetsov, Z. Luo, K. I. Hardcastle, C. L. Hill, *Science* **2010**, *328*, 342 – 345.
[34] D. K. Dogutan, R. McGuire, Jr., D. G. Nocera, *J. Am. Chem. Soc.* **2011**, *133*, 9178 – 9180.
[35] N. S. McCool, D. M. Robinson, J. E. Sheats, G. C. Dismukes, *J. Am. Chem. Soc.* **2011**, *133*, 11446 – 11449.
[36] D. Hong, J. Jung, J. Park, Y. Yamada, T. Suenobu, Y.-M. Lee, W. Nam, S. Fukuzumi, *Energy Environ. Sci.* **2012**, *5*, 7606.
[37] W. C. Ellis, N. D. McDaniel, S. Bernhard, T. J. Collins, *J. Am. Chem. Soc.* **2010**, *132*, 10990 – 10991.
[38] D. Hong, S. Mandal, Y. Yamada, Y. M. Lee, W. Nam, A. Llobet, S. Fukuzumi, *Inorg. Chem.* **2013**, *52*, 9522 – 9531.
[39] C. Panda, J. Debgupta, D. Diaz Diaz, K. K. Singh, S. Sen Gupta, B. B. Dhar, *J. Am. Chem. Soc.* **2014**, *136*, 12273 – 12282.
[40] S. M. Barnett, K. I. Goldberg, J. M. Mayer, *Nat. Chem.* **2012**, *4*, 498 – 502.
[41] Z. Chen, T. J. Meyer, *Angew. Chem. Int. Ed.* **2013**, *52*, 700 – 703; *Angew. Chem.* **2013**, *125*, 728 – 731.
[42] M. T. Zhang, Z. Chen, P. Kang, T. J. Meyer, *J. Am. Chem. Soc.* **2013**, *135*, 2048 – 2051.
[43] T. Zhang, C. Wang, S. Liu, J. L. Wang, W. Lin, *J. Am. Chem. Soc.* **2014**, *136*, 273 – 281.
[44] P. Garrido-Barros, I. Funes-Ardoiz, S. Drouet, J. Benet-Buchholz, F. Maseras, A. Llobet, *J. Am. Chem. Soc.* **2015**, *137*, 6758 – 6761.
[45] G. C. Dismukes, R. Brimblecombe, G. A. N. Felton, R. S. Pryadun, J. E. Sheats, L. Spiccia, G. F. Swiegers, *Acc. Chem. Res.* **2009**, *42*, 1935 – 1943.
[46] J. N. Israelachvili, D. J. Mitchell, B. W. Ninham, *J. Chem. Soc. Faraday Trans. 2* **1976**, *72*, 1525 – 1568.
[47] H. Ringsdorf, B. Schlarb, J. Venzmer, *Angew. Chem. Int. Ed. Engl.* **1988**, *27*, 113 – 158; *Angew. Chem.* **1988**, *100*, 117 – 162.
[48] X. Zhang, C. Wang, *Chem. Soc. Rev.* **2011**, *40*, 94 – 101.
[49] C. Wang, Z. Wang, X. Zhang, *Acc. Chem. Res.* **2012**, *45*, 608 – 618.
[50] L.-B. Xing, S. Yu, X.-J. Wang, G.-X. Wang, B. Chen, L.-P. Zhang, C.-H. Tung, L.-Z. Wu, *Chem. Commun.* **2012**, *48*, 10886 – 10888.
[51] N. Planas, L. Vigara, C. Cady, P. Miró, P. Huang, L. Hammarström, S. Styring, N. Leidel, H. Dau, M. Haumann, L. Gagliardi, C. J. Cramer, A. Llobet, *Inorg. Chem.* **2011**, *50*, 11134 – 11142.
[52] A. C. Dengel, W. P. Griffith, *Inorg. Chem.* **1991**, *30*, 869 – 871.
[53] K. J. LaChance-Galang, P. Doan, M. J. Clarke, U. Rao, A. Yamano, B. M. Hoffman, *J. Am. Chem. Soc.* **1995**, *117*, 3529 – 3538.
[54] X.-J. Wang, L.-B. Xing, F. Wang, G.-X. Wang, B. Chen, C.-H. Tung, L.-Z. Wu, *Langmuir* **2011**, *27*, 8665 – 8671.

Received: February 16, 2016
Published online: April 13, 2016

